Aerodynamic Performance Enhancement of a River Ship by Using CFD

He Van Ngo * , Bui Thanh Danh , Hoang Cong Liem , Le Duy An

Posted Date: 8 September 2025

doi: 10.20944/preprints202509.0592.v1

Keywords: river ship; hydrodynamic resistance; aerodynamic; CFD; hull; wind drag

 doi:10.20944/preprints202509.0592.v1

Article

Aerodynamic Performance Enhancement of a River Ship by Using CFD

Ngo Van He [1,*], Le Duy An [2], Bui Thanh Danh [1,3] and Hoang Cong Liem [1]

[1] School of Mechanical Engineering, Hanoi University of Science and Technology
[2] Delta Global School, Tay Ho, Hanoi, Vietnam
[3] Shipbuilding Faculty, Vietnam Maritime University, Haiphong, Vietnam
* Correspondence: he.ngovan@hust.edu.vn;

Abstract

The aerodynamic performance of river ships, particularly cargo river ships operating in inland waterways, plays a crucial role in determining their efficiency, safety, and economic viability. While traditional ship design has primarily focused on optimizing hull forms to minimize resistance acting on the ship, recent research highlights the growing importance of aerodynamic considerations, especially for ships with large accommodation above the water surface. This study synthesizes recent investigations on aerodynamic improvements achieved through the optimization of hull and accommodation for ships using Computational Fluid Dynamics (CFD). Pressure distribution analyses reveal that high-pressure zones around the hull significantly contribute to wind drag. Advanced CFD simulations, employing Reynolds-Averaged Navier–Stokes (RANS) methods, demonstrate notable reductions in wind drag through targeted modifications of ship accommodation. The results confirm that such design improvements of river ship accommodation can reduce wind drag acting on the ship, leading to lower fuel consumption, improved stability, and enhanced operational safety.

Keywords: river ship; hydrodynamic resistance; aerodynamic; CFD; hull; wind drag.

1. Introduction

Improving the energy efficiency of cargo ships has become a central objective in modern marine transportation, with the reduced resistance acting on the ship representing a key component of this effort [1–5]. While wind drag is typically the dominant factor in a ship's total resistance, ships with large projected area above the waterline may experience significant wind drag, which in some cases constitutes a considerable proportion of the total resistance. For instance, a fully loaded container ship encountering headwinds can have wind drag accounting for nearly 10% of its total resistance. Inland waterway cargo ships, which are widely operated in Vietnam, often feature pronounced accommodation and wide, flat decks, resulting in a high windage area. Consequently, wind drag becomes especially critical for river ships, directly influencing fuel consumption, maneuverability, and operational safety under strong wind conditions.

Traditionally, standard ship design methodologies have primarily focused on refining hull shapes to minimize wind drag, often neglecting aerodynamic influences. The above-water hull, such as deckhouses, accommodation are generally engineered for functional and stability criteria, with minimal aerodynamic optimization. In numerous instances, the wind load was regarded as a minor consideration, constituting merely a few percent of the total resistance under mild conditions. Nonetheless, as the demand for enhanced fuel efficiency and reduced emissions increases, there is a growing acknowledgment that wind drag acting on the accommodation must not be overlooked for high-windage ships. Blunt-fronted structures and protruding cargo, such as container stacks, can

 doi:10.20944/preprints202509.0592.v1

function as sails in the wind, generating considerable drag that increases fuel consumption and adversely affects handling in crosswinds.

In recent years, various studies have examined methods to mitigate wind drag acting on ships' hulls and accommodation. Wind tunnel experiments and Computational Fluid Dynamics (CFD) models have been extensively utilized to examine ship aerodynamics. CFD, in particular, has proven to be a reliable tool for evaluating aerodynamic performance with good agreement with experimental results [1–4,6,7]. A focus of many studies has been on large ocean ships like container ships, which have extensive above-water hulls. Researchers have found that smoothing or streamlining the external shape of these ships can yield substantial wind drag reductions. Andersen et al. showed that an optimized container stacking configuration by presenting a smoother face to the wind significantly lowers wind forces on a 900 TEU container ship [1]. Kim et al. likewise tested various add-on devices on a container ship's accommodation, such as gap protectors between container stacks and bow visors, and reported wind drag reductions up to 56% in certain headwind conditions [8]. Other modifications, including fitting side covers along the deck edges or adding a dome-shaped fairing at the bow, have been shown to cut the wind drag by roughly 30–40% [2,8]. These findings underscore that relatively simple design changes to the above-water hull can markedly improve a ship's aerodynamic performance.

Beyond container carriers, studies have extended to ships with large accommodations, such as passenger vessels and specialty ships. Wind drag acting on high-profile passenger ships such as ro-ro ferries or cruise liners is a critical concern, and recent CFD analyses and wind tunnel tests confirm that aerodynamic performance optimizations can yield significant. Research by Ngo et al. examined a passenger ship with a tall frontal accommodation and proposed redesigned bow shapes that substantially reduced wind drag [3]. In other research, Ngo et al. have conducted a series of studies on hull accommodation interaction effects [4,9]. Their work on a wood-chip carrier demonstrated that reshaping the accommodation block and adding features like side guards can lessen the adverse interaction and lower the overall wind resistance acting on the ship. Related investigations by other authors have similarly confirmed that modifying the geometry of the accommodation or adding appendages can lead to appreciable reductions in wind forces on the hull [9,10]. Collectively, these works highlight that both the shape of a ship's exposed profile and its heading relative to the oncoming wind are critical factors governing wind drag.

Despite the growing body of research on ship aerodynamics, relatively little attention has been given to inland waterway cargo ships. River ships often operate at lower speeds and in confined channels, yet they frequently encounter strong crosswinds over open stretches, making them susceptible to wind drag and lateral drift. In this study, we address this gap by evaluating the aerodynamic performance of a typical Vietnamese river cargo ship and analyzing how various orientations affect the pressure distribution around the ship. We employ CFD simulations using ANSYS Fluent version 19.2 with a RANS k–ε turbulence viscous model to compute the wind drag and pressure distribution acting on the hull and accommodation of the ship. By examining various wind angles and conditions, we identify the areas of high pressure and flow separation around the accommodation that contribute most to wind drag. The overall objective is to quantify the potential drag reduction from these design modifications and thereby demonstrate how aerodynamic refinement of the superstructure can improve the energy efficiency of river ships. This research contributes new knowledge on aerodynamic optimization for inland vessels, a topic that has seen limited study, and the findings can inform future ship design standards and retrofitting strategies for better performance in Vietnam's inland waterway fleet.

 doi:10.20944/preprints202509.0592.v1

Figure 1. River cargo ship operated on the inland waterway of northern Vietnam

2. Methodology

2.1. River Ship Model

In this study, a representative river cargo ship, commonly operated on the waterways of northern Vietnam, is selected as the reference model. Figure 2 illustrates the body plan of the ship and accommodation. The principal particulars of the ship are summarized in Table 1.

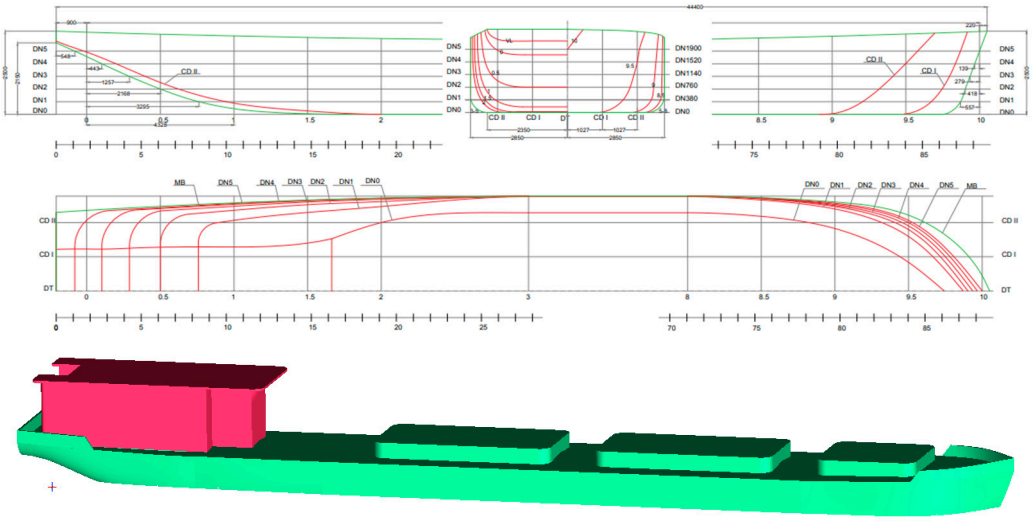

Figure 2. Body plan of the traditional river cargo ship in Vietnam

 doi:10.20944/preprints202509.0592.v1

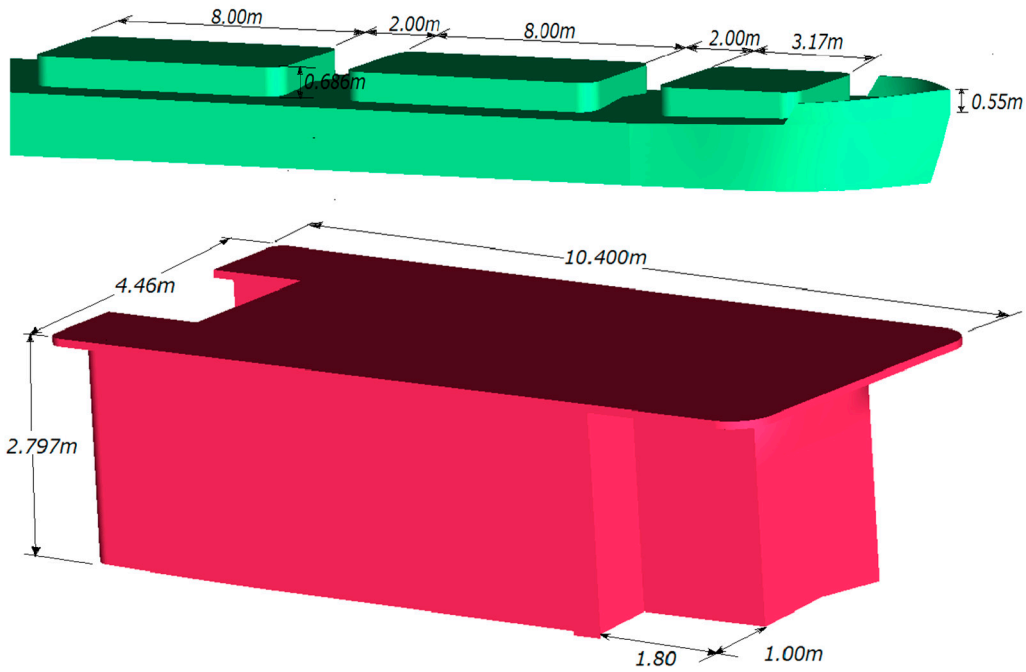

Figure 3. Accommodation of the original river cargo ship

Table 1. Principal dimensions of the ship

Parameters	Value	Unit
Length, L	43.25	m
Breadth, B	5.70	m
Depth, H	2.25	m
Draft, d	1.90	m
Frontal projected area, S_x	21.64	m^2
Lateral projected area, S_y	110.79	m^2
Displacement, D	436.27	ton
Block coefficient, C_b	0.9162	-
Waterline coefficient, C_W	0.8621	-
Midship coefficient, C_M	0.9683	-

2.2. Numerical Setup

In CFD simulations, the Reynolds-Averaged Navier–Stokes (RANS) equations are among the most widely applied approaches. The detailed methodologies and governing equations for numerical modeling have been extensively described in previous studies [1,3,6,7,11,12]. In this research, the aerodynamic performances of the ship are analyzed using the commercial CFD package ANSYS Fluent v.19.2, employing the k–ε turbulence viscous model [13–15]. The computational domain was defined with dimensions of 6.5L in length, L in width, and L in height, where L denotes the ship length. For this research, with an actual ship length of 43.25 m, the domain dimensions were determined as 200 m in length, 40 m in width, and 40 m in height. The domain was discretized using an unstructured mesh consisting of approximately 2.683 million cells.

Boundary conditions were imposed corresponding to wind velocities ranging from Beaufort level 1 to level 5, which represent Reynolds numbers between 6×10^6 and 2.2×10^7. The detailed input parameters are summarized in Table 2, and Figure 4 illustrates the computational domain and the mesh configuration.

 doi:10.20944/preprints202509.0592.v1

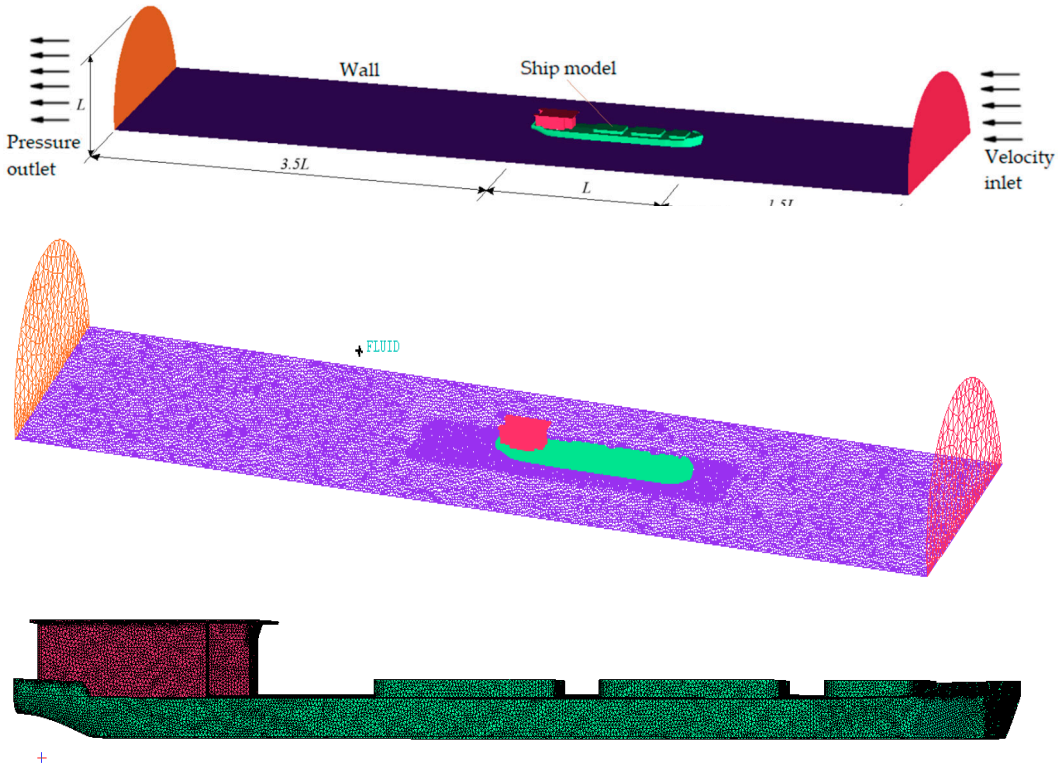

Figure 4. Computational domain and mesh

Table 2. Computational conditions

Conditions	Parameters	Unit
Velocity inlet, V	2.57 – 9.26	m/s
Pressure outlet, p	1.025	at
Reynold, R_n	6×10^6 - 2.2×10^7	-
Air density, ρ	1.225	kg/m^3
Air kinematic viscosity, ν	1.7894×10^{-5}	kg/m·s

In CFD simulations, each step of the modeling process can significantly influence the results. To obtain reliable results, all stages of the computation must strictly follow validated guidelines and best practices documented in authoritative references [2,5,7,9,16–19]. Moreover, the accuracy of numerical predictions can be verified by comparing the simulation results with experimental model tests or benchmark data from recognized studies. Grid convergence assessment, together with prior experience in applying CFD to similar problems, also serves as an important approach to evaluate the reliability of the simulation results [2–4,9,20,21].

In this study, a mesh convergence analysis was conducted using seven different mesh numbers, with corresponding y^+ values ranging from 4.786 to 128.262. The simulations were carried out under identical boundary conditions, with a flow velocity corresponding to a Reynolds number of $R_n = 6.26 \times 10^6$. Table 3 and Figure 5 present the comparison of wind drag acting on the ship for the different mesh configurations. The results confirm that the selected mesh provides sufficient numerical accuracy and stability for the CFD simulations.

Table 3. Wind drag acting on the ship in different mesh numbers, at $R_n=6.26 \times 10^6$.

Mesh Number	y+	C_d	ΔC_d, %

 doi:10.20944/preprints202509.0592.v1

(×10⁶)			
1.1535	128.262	0.9891	2.6319
1.6246	81.235	0.9675	0.4599
2.2356	43.768	0.9645	0.1461
3.1655	30.756	0.9637	0.0669
3.8633	17.658	0.9635	0.0466
5.7366	9.835	0.9632	0.0160
7.6826	4.786	0.9631	0.0000

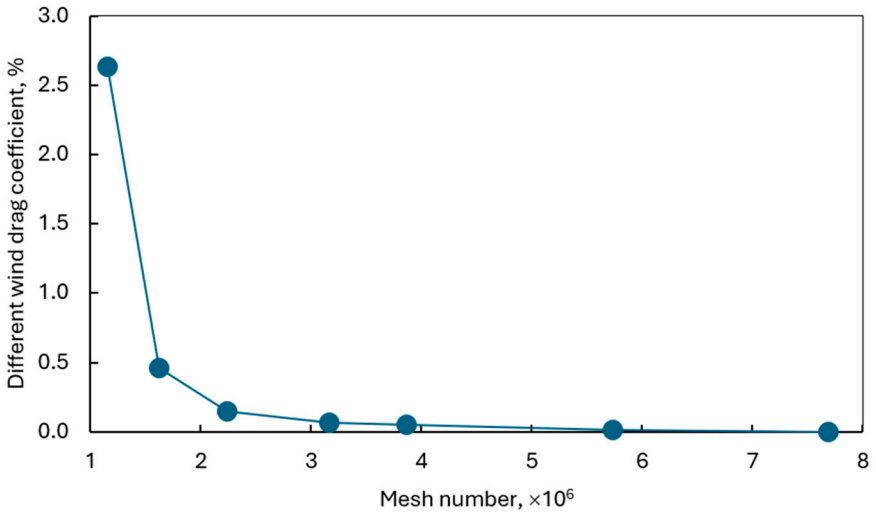

Figure 5. Effect of mesh number on wind drag acting on the ship in head wind, at $R_n=6.26\times10^6$

The comparison of wind drag coefficients acting on the ship, as illustrated in Figure 5, indicates that the deviation resulting from varying the mesh density in the investigated region remains below 2.63%. As the y+ value decreases, the deviation is significantly reduced, reaching below 0.5%. These results confirm the mesh convergence and provide a reliable basis for the subsequent numerical simulations conducted in this study.

2.3. Results of Aerodynamic Performance Acting on the Original River Cargo Ship

Based on the calculation of the aerodynamic performances of the original model, Figure 6 shows the results of the pressure distribution around the hull and wind drag acting on the ship in the different Reynolds numbers. The pressure distribution around and over the hull surface of the ships shows that the bow shape and the accommodation have higher-pressure areas than other areas. Thus, the concentration of pressure areas occurs in areas with large and sharply changing wind surfaces on the hull. These are the areas that may need to be improved in design to reduce the area of this high-pressure area. The pressure exerted on the hull causes wind drag, so it is essential to reduce the areas of high pressure during the ship's design process. In addition, it is possible to change the ship's operating posture or adjust the wind direction acting on the ship to control and change the areas of high pressure acting on the ship, helping to reduce the wind drag acting on the ship.

Preprints.org (www.preprints.org) | NOT PEER-REVIEWED | Posted: 8 September 2025 doi:10.20944/preprints202509.0592.v1

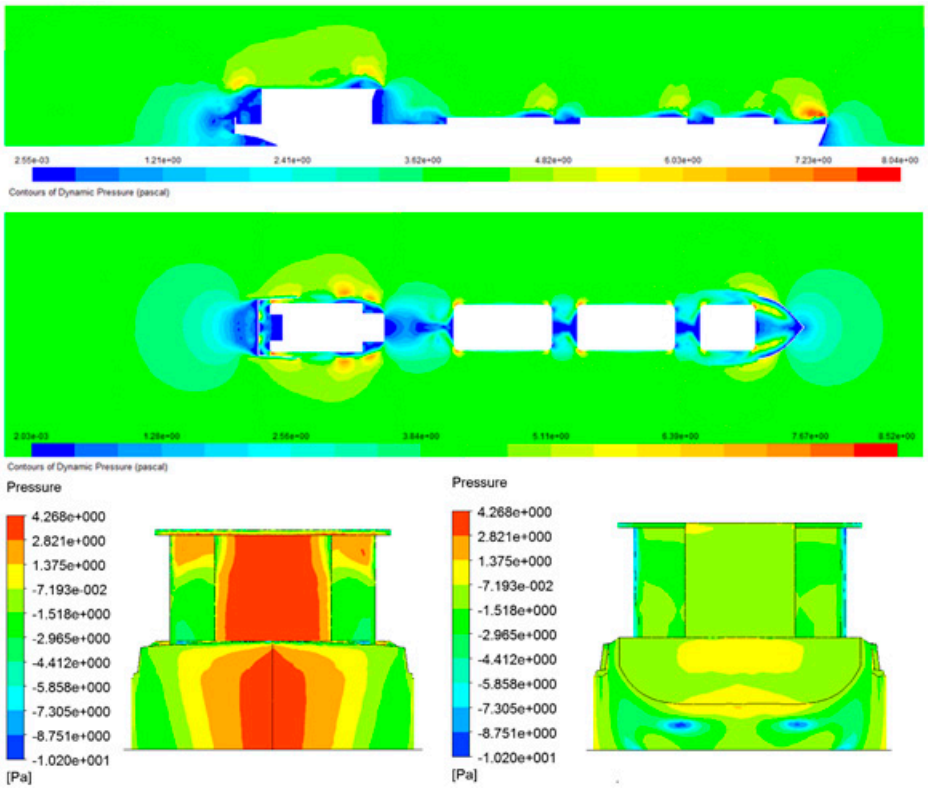

a) $R_n = 6.20 \times 10^6$

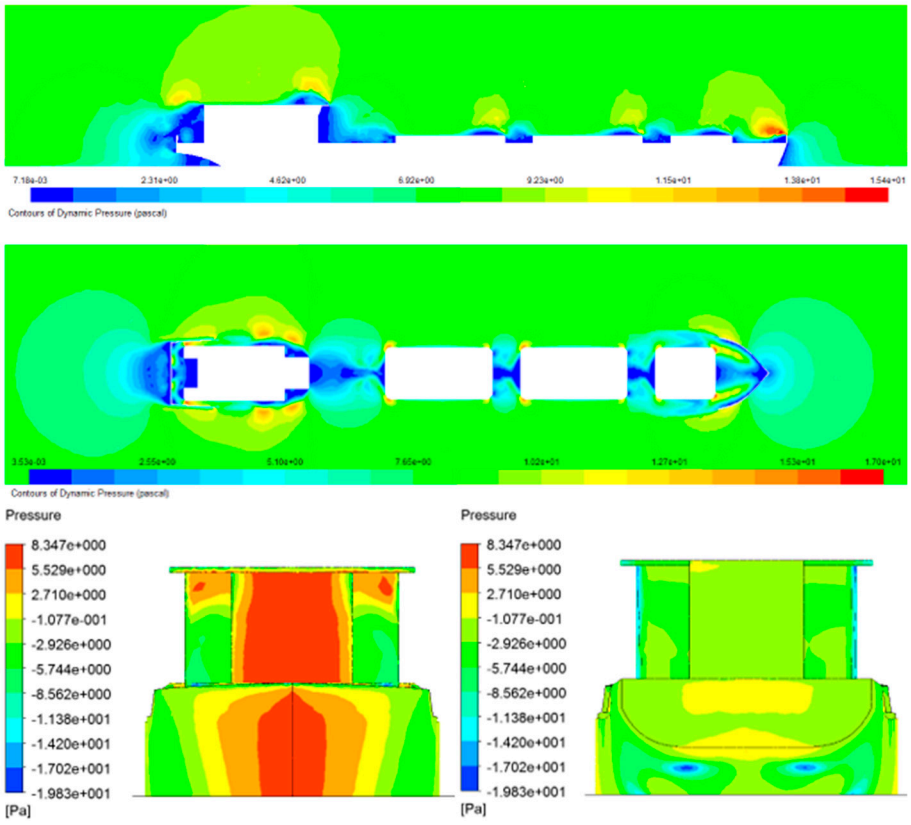

b) $R_n = 8.67 \times 10^6$

 doi:10.20944/preprints202509.0592.v1

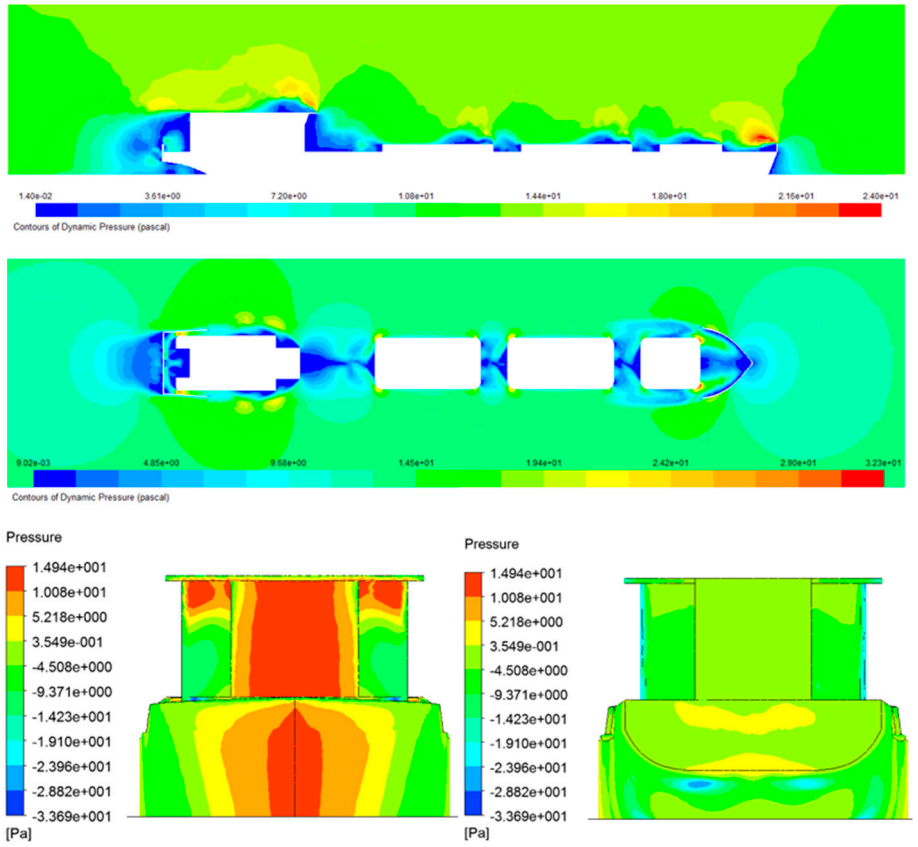

c) $R_n = 11.20 \times 10^6$

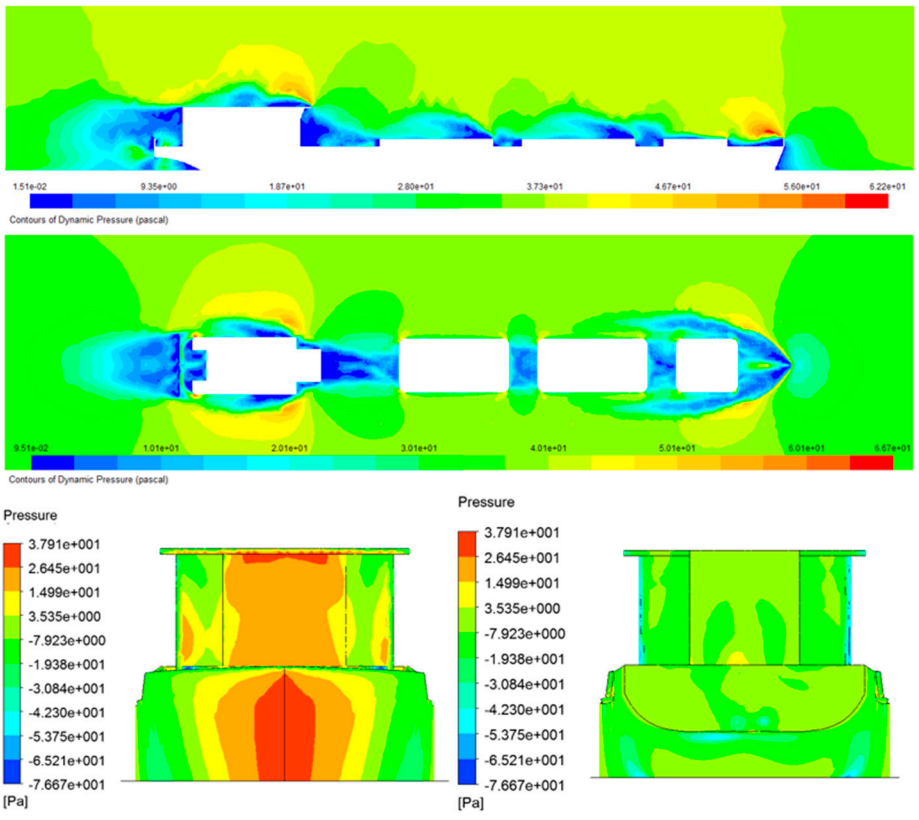

d) $R_n = 13.60 \times 10^6$

Preprints.org (www.preprints.org) | NOT PEER-REVIEWED | Posted: 8 September 2025 doi:10.20944/preprints202509.0592.v1

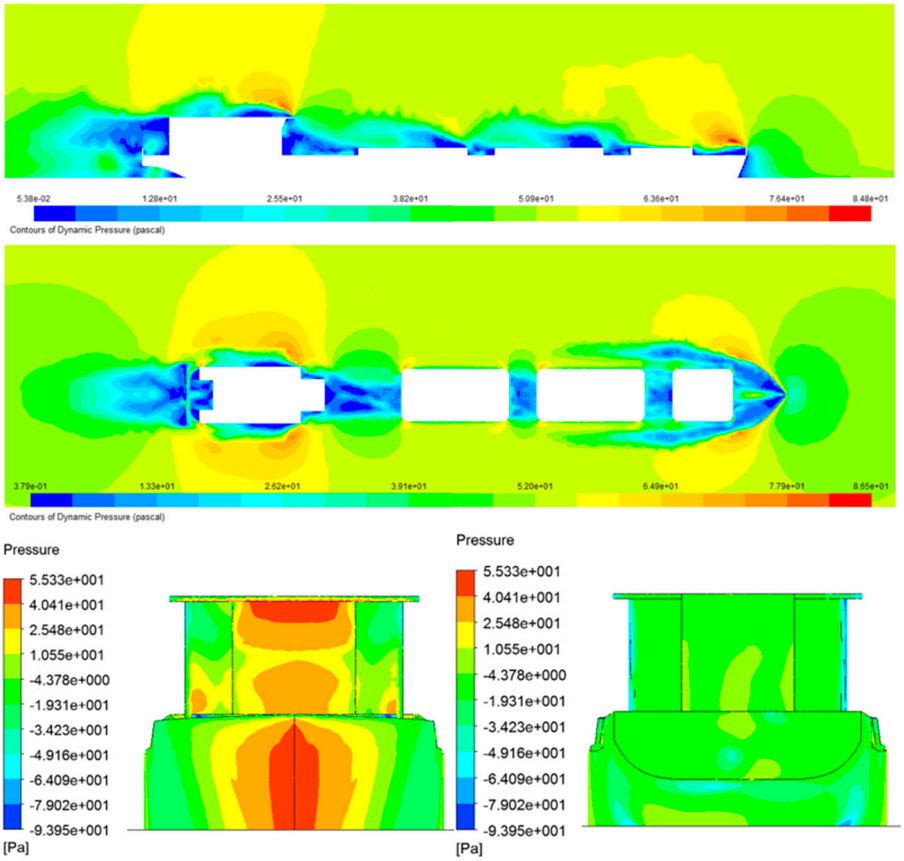

e) $R_n = 18.60 \times 10^6$

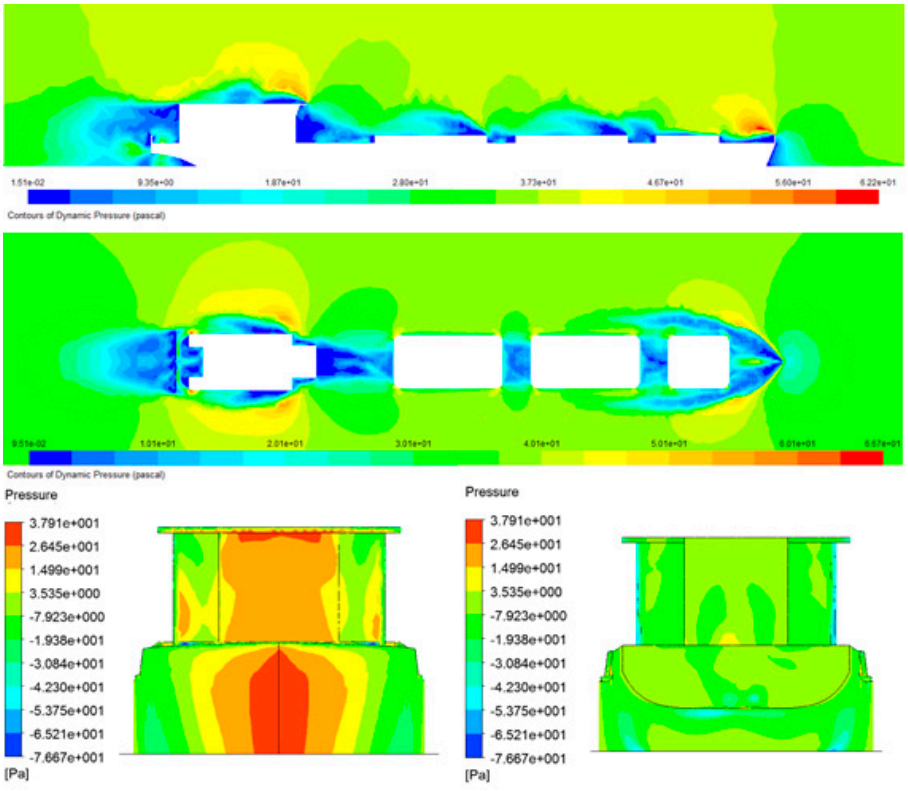

f) $R_n = 22.30 \times 10^6$

Figure 6. Pressure distribution around the hull and over the hull surface of the ship

Preprints.org (www.preprints.org) | NOT PEER-REVIEWED | Posted: 8 September 2025 doi:10.20944/preprints202509.0592.v1

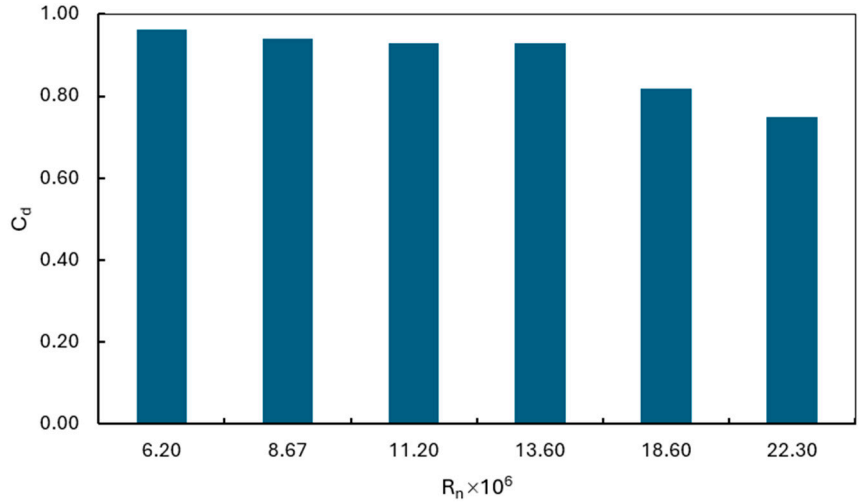

Figure 7. Wind drag coefficient acting on the ship

Figure 7 shows that as the speed increases, the wind drag coefficient acting on the ship tends to decrease. In the speed range corresponding to Reynolds numbers below 18.6 x 10^6, the wind drag coefficient acting on the hull tends to stabilize and change less than when the speed increases beyond the Reynolds limit of 18.6 × 10^6. The results of wind drag acting on the ship surveyed above are consistent with the CFD calculation results obtained on the pressure distribution and flow around the ship, as shown. Table 4 shows the detailed wind drag acting on the ship.

Table 4. Wind drag acting on the ship corresponds to the Reynolds number.

$R_n \times 10^6$	$R_{d(p)}$, N	$R_{d(f)}$, N	R_d, N	$C_{d(p)}$	$C_{d(f)}$	C_d
6.20	79.1056	5.3631	84.4686	0.9018	0.0611	0.9632
8.67	152.0577	9.6966	161.7544	0.8844	0.0564	0.9411
11.20	249.2042	14.6588	263.8630	0.8769	0.0516	0.9287
13.60	374.7486	20.2532	395.0018	0.8827	0.0477	0.9306
18.60	612.9621	33.3372	646.2994	0.7764	0.0422	0.8189
22.30	807.5041	45.7045	853.2086	0.7103	0.0402	0.7507

In the calculation, the wind drag coefficient is defined as:

$$C_d = \frac{R_d}{0.5\rho V^2 S_x} \quad (1)$$

$$C_d = C_{d(f)} + C_{d(p)} \quad (2)$$

Where: C_d is the total wind drag coefficient
$C_{d(f)}$ is the component of the frictional viscous wind drag
$C_{d(p)}$ is the component of the pressure viscous wind drag
R_d is the total wind drag acting on the ship, N
V is the velocity of the ship, m/s

3. Effect of Ship Operating Attitude on Aerodynamic Performances

In this section, the effect of the ship's operating attitude on its aerodynamic performance and the wind drag acting on the vessel is comparatively analyzed. The objective is to clarify how operating attitude influences wind drag and to assess the potential for reducing wind drag through attitude adjustment. Two scenarios are considered: the ship operating in a balanced condition with a 0° bow angle, and the ship operating with a 3° bow angle. Aerodynamic performance is evaluated for both cases across the ship's operating speed range, corresponding to wind levels from 1 to 5. Figure 8 shows a model of the ship in computation.

Preprints.org (www.preprints.org) | NOT PEER-REVIEWED | Posted: 8 September 2025 doi:10.20944/preprints202509.0592.v1

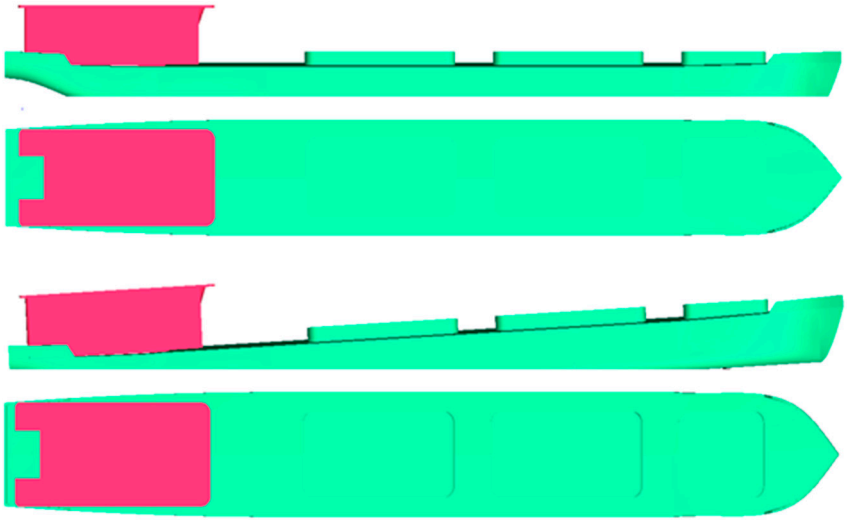

Figure 8. Ship model used in the study of the influence of ship attitude with bow pitch angles of 0 and 3 degrees

Figure 9 presents the simulation results of the pressure distribution around the hull when the ship operates with a 3° bow angle. Compared to the balanced position (0° bow angle), the high-pressure region on the bow surface increases, while part of the high-pressure area on the accommodation decreases due to the effect of the bow angle. These changes in pressure distribution directly influence the wind drag acting on the hull.

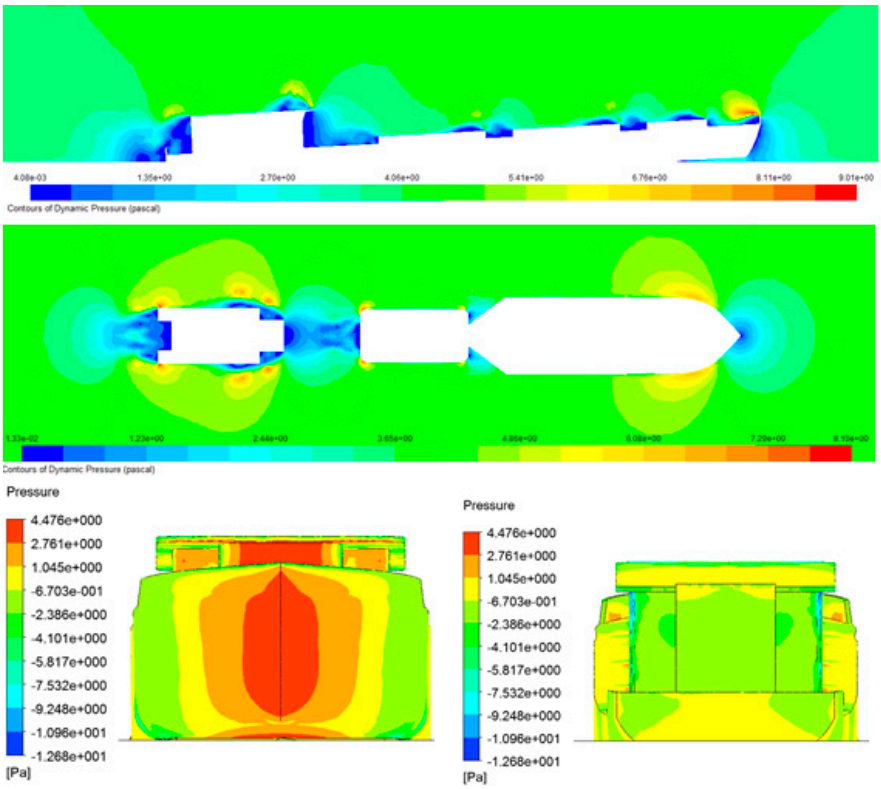

a) $R_n = 6.20 \times 10^6$

 doi:10.20944/preprints202509.0592.v1

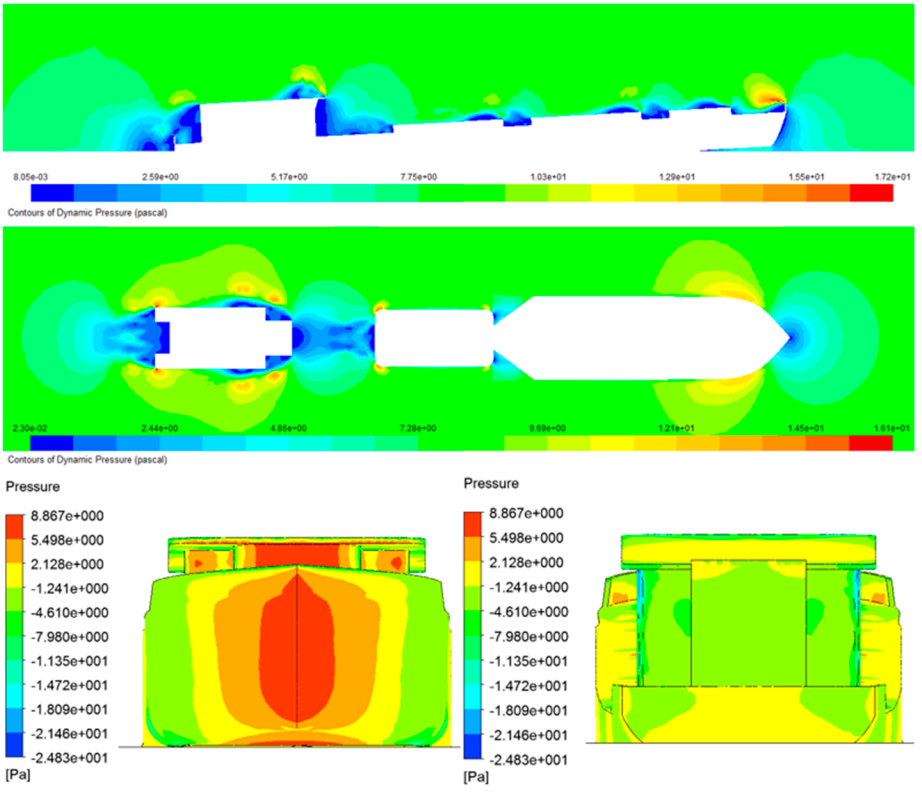

b) $R_n = 8.67 \times 10^6$

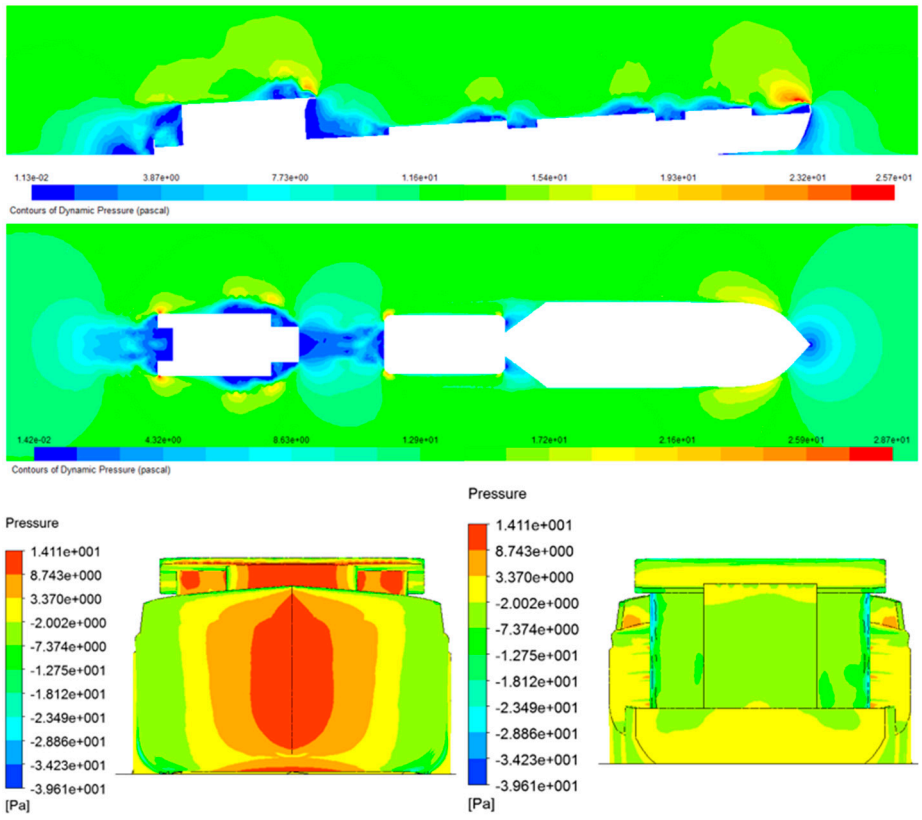

c) $R_n = 11.20 \times 10^6$

Preprints.org (www.preprints.org) | NOT PEER-REVIEWED | Posted: 8 September 2025 doi:10.20944/preprints202509.0592.v1

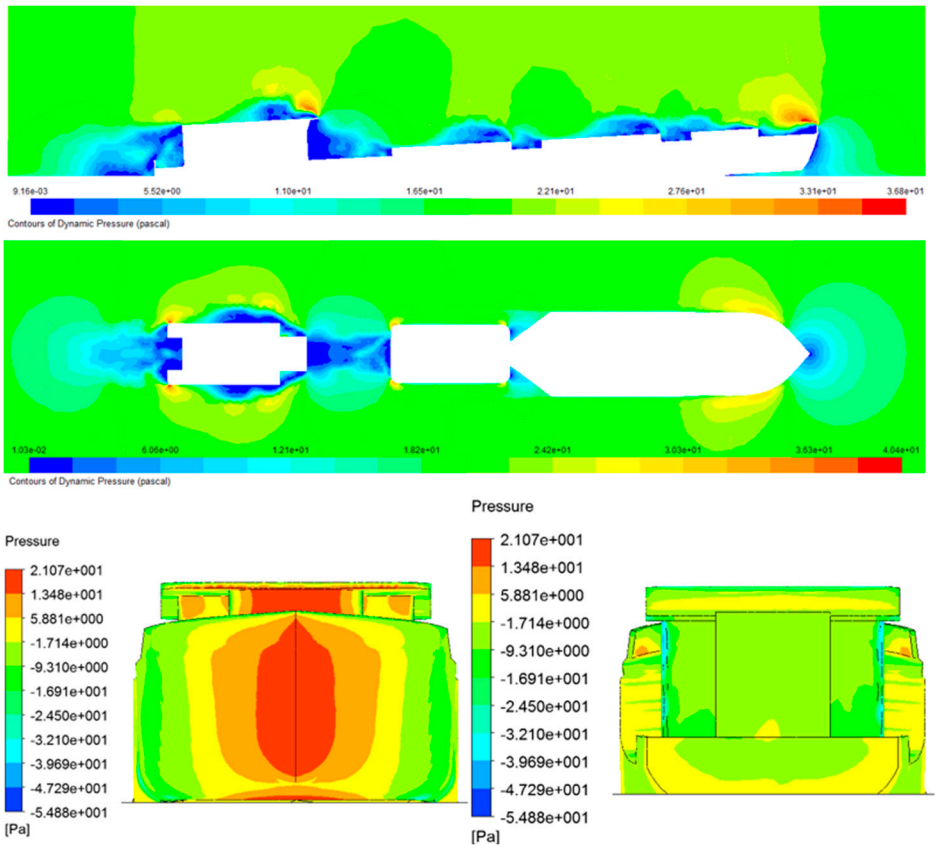

d) $R_n = 13.60 \times 10^6$

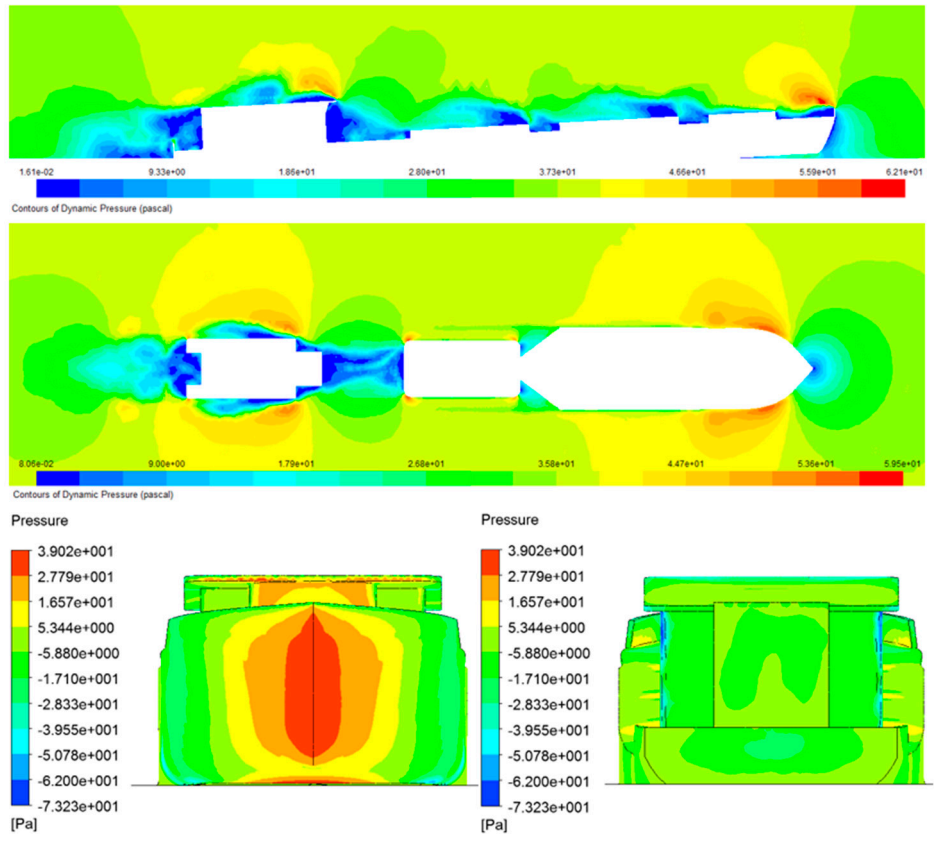

e) $R_n = 18.60 \times 10^6$

 doi:10.20944/preprints202509.0592.v1

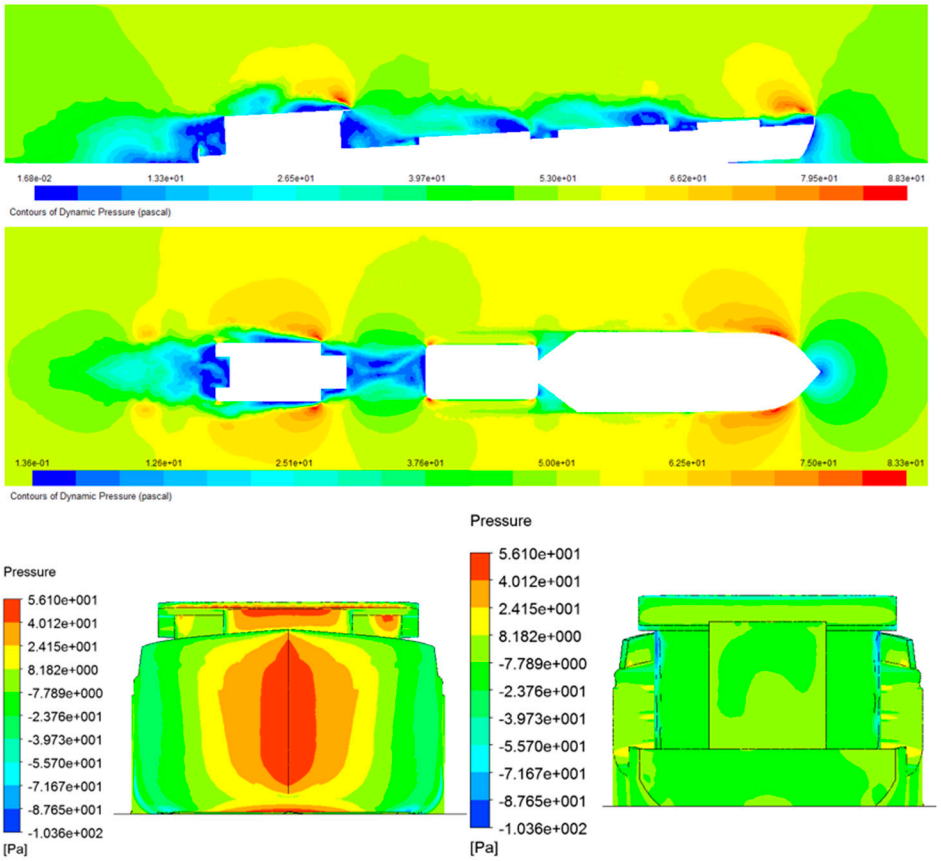

f) $R_n = 22.30 \times 10^6$

Figure 9. Pressure distribution around the hull and over the hull surface of the ship with a 3-degree bow angle operating condition.

Figure 10 compares the wind drag between the balanced position and the 3° bow angle cases. At low speeds ($R_n < 8.67 \times 10^6$), the wind drag components are nearly identical in both cases. As the speed increases, differences become more noticeable, with a maximum of up to 10%. In the intermediate range ($R_n = 11.2 \times 10^6$ to 22.30×10^6), the 3° bow angle reduces the total wind drag acting on the ship by roughly 10% compared to the balanced position.

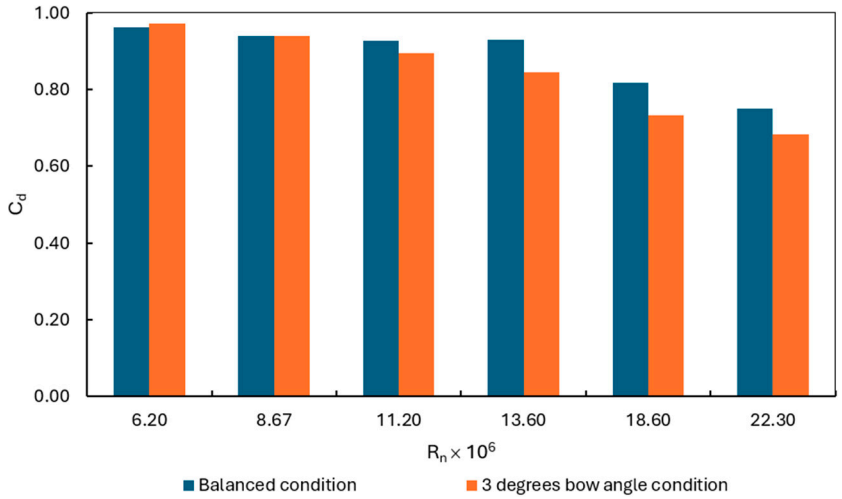

Figure 10. Wind drag acting on the hull in the balanced condition and the 3-degree bow angle condition

In practice, research on ship design indicates that the vessel's operating posture has a significant influence on its stability and balance. Therefore, to ensure safety, the ship must not only be operated in a posture that

 doi:10.20944/preprints202509.0592.v1

minimizes wind drag acting on the hull but also in one that maintains sufficient stability and balance, thereby safeguarding both crew and cargo. The results show that to reduce the wind drag acting on the ship, we can develop a new accommodation for the ship to minimize the effect on its aerodynamic performance during transportation. Tables 5 and 6 show the detailed wind drag acting on the ship in the 3-degree bow angle condition, and compare with those of the balanced condition.

Table 5. Wind drag acting on the ship in the 3-degree bow angle condition.

$R_n \times 10^6$	$R_{d(p)}$, N	$R_{d(f)}$, N	R_d, N	$C_{d(p)}$	$C_{d(f)}$	C_d
6.20	79.7980	5.3979	85.1959	0.9099	0.0616	0.9715
8.67	151.6999	9.7662	161.4661	0.8826	0.0568	0.9394
11.20	239.5849	14.8093	254.3942	0.8432	0.0521	0.8953
13.60	338.3394	20.6182	358.9576	0.7971	0.0486	0.8457
18.60	544.7182	34.6321	579.3502	0.6902	0.0439	0.7340
22.30	729.9862	46.4016	776.3879	0.6423	0.0408	0.6831

Table 6. Comparison of wind drag acting on the ship in the different operating conditions.

$R_n \times 10^6$	Wind drag, %			Wind drag coefficient, %		
	$R_{d(p)}$	$R_{d(f)}$	R_d	$C_{d(p)}$	$C_{d(f)}$	C_d
6.20	0.88	0.65	0.86	0.88	0.65	0.86
8.67	-0.24	0.72	-0.18	-0.24	0.72	-0.18
11.20	-3.86	1.03	-3.59	-3.86	1.03	-3.59
13.60	-9.72	1.80	-9.13	-9.72	1.80	-9.13
18.60	-11.13	3.88	-10.36	-11.13	3.88	-10.36
22.30	-9.60	1.53	-9.00	-9.60	1.53	-9.00

The results indicate that the frictional viscous wind drag component acting on the ship remains nearly identical under both operating conditions, with a difference of less than 3.88%. In contrast, the pressure-induced wind drag component shows a clear variation, as presented in Table 6. This discrepancy is likely attributable to differences in the pressure and velocity distributions around the ship under the two operating conditions.

4. Conclusions

This study investigated the influence of ship operational orientation on the aerodynamic performances and wind drag exerted on a typical Vietnamese river cargo ship. Using CFD simulations based on the RANS k-ε turbulence model, we evaluated pressure distributions and wind drag acting on the ship under different operating attitudes, particularly comparing a balanced position (0° bow pitch) with a slightly pitched position (3° bow angle).

The results show that high-pressure zones are concentrated around the bow and the front face of the accommodation, acting as primary contributors to overall wind drag. When the ship operates with a 3-degree bow angle orientation, the high-pressure region around the accommodation was reduced, although pressure near the bow increased. Across the surveyed Reynolds number range (6.2×10^6 to 22.3×10^6), wind drag decreased by up to 10% in the 3-degree pitched configuration compared to the balanced position, particularly in the mid-to-high speed range ($Rn > 11.2 \times 10^6$). These findings confirm that small changes in operational orientation can positively affect aerodynamic performance.

Although the wind drag reduction was modest, it is practically significant given the simplicity and feasibility of implementing such changes without requiring structural modifications. However, these adjustments must be evaluated alongside ship stability and safety constraints. Future research should explore a broader range of operational configurations and combine aerodynamic analysis with dynamic stability assessments to optimize both resistance reduction and safe maneuverability in riverine environments.

 doi:10.20944/preprints202509.0592.v1

Author Contributions: Conceptualization, N.V.He, L.D.An; methodology, N.V.He, H.C.Liem and B.T. Danh; software, B.T. Danh, H.C.Liem and L.D.An; validation, N.V.He, L.D.An; writing—original draft preparation, N.V.He, L.D.An and B.T.Danh; writing—review and editing N.V.He, H.C.Liem; supervision, N.V.He; project administration, N.V.He. All authors have read and agreed to the published version of the manuscript.

Funding: Hanoi University of Science and Technology (HUST).

Acknowledgments: This research is funded by Hanoi University of Science and Technology (HUST) under project number T2023-PC-015. The authors would like to warmly express their thanks for the support.

Conflicts of Interest: The authors declare no conflict of interest.

References

1. Andersen, I.M.V., *Wind loads on post-panamax container ship.* Ocean engineering, 2013. **58**: p. 115-134.
2. Van He, N., K. Mizutani, and Y. Ikeda, *Reducing air resistance acting on a ship by using interaction effects between the hull and accommodation.* Ocean engineering, 2016. **111**: p. 414-423.
3. Van He, N., N. Van Hien, and N.-T. Bui, *Analyis of aerodynamic performance of passenger ship with different frontal accommodations using CFD.* Ocean engineering, 2023. **270**: p. 113622.
4. He, N.V., et al., *Interaction effect between hull and accommodation on wind drag acting on a container ship.* Journal of Marine Science and Engineering, 2020. **8**(11): p. 930.
5. Fujiwara, T., et al. *Experimental investigation and estimation on wind forces for a container ship*. in *ISOPE International Ocean and Polar Engineering Conference*. 2009. ISOPE.
6. Wang, P., F. Wang, and Z. Chen, *Investigation on aerodynamic performance of luxury cruise ship.* Ocean Engineering, 2020. **213**: p. 107790.
7. Janssen, W., B. Blocken, and H. van Wijhe, *CFD simulations of wind loads on a container ship: Validation and impact of geometrical simplifications.* Journal of wind engineering and industrial aerodynamics, 2017. **166**: p. 106-116.
8. Kim, Y., et al. *Design and performance evaluation of superstructure modification for air drag reduction of a container ship*. in *ISOPE International Ocean and Polar Engineering Conference*. 2015. ISOPE.
9. Van He, N., K. Mizutani, and Y. Ikeda, *Effects of side guards on aerodynamic performances of the wood chip carrier.* Ocean engineering, 2019. **187**: p. 106217.
10. Toan, N.C. and N. Van He, *Effect of hull and accommodation shape on aerodynamic performances of a small ship.* Vietnam Journal of Marine Science and Technology, 2018. **18**(4): p. 413-421.
11. Zhou, L., et al., *Computational fluid dynamic (CFD)*, in *Discrete Element Method for Multiphase Flows with Biogenic Particles: Agriculture Applications*. 2024, Springer. p. 65-82.
12. Bhaskaran, R. and L. Collins, *Introduction to CFD basics.* Cornell University-Sibley School of Mechanical and Aerospace Engineering, 2002: p. 1-21.
13. Sodja, J. and R. Podgornik, *Turbulence models in CFD.* University of Ljubljana, 2007: p. 1-18.
14. Piquet, J., *Turbulent flows: models and physics*. 2013: Springer Science & Business Media.
15. Collie, S., M. Gerritsen, and P. Jackson, *A review of turbulence modelling for use in sail flow analysis*. 2001: Department of Engineering Science, University of Auckland Auckland, New Zealand.
16. Wnęk, A. and C.G. Soares, *CFD assessment of the wind loads on an LNG carrier and floating platform models.* Ocean engineering, 2015. **97**: p. 30-36.
17. Viola, I.M., *Downwind sail aerodynamics: A CFD investigation with high grid resolution.* Ocean engineering, 2009. **36**(12-13): p. 974-984.
18. Van He, N., *Effect of mesh on CFD aerodynamic performances of a container ship.* Vietnam Journal of Marine Science and Technology, 2020. **20**(3): p. 343-353.
19. Watanabe, I., et al. *A study on reduction of air resistance acting on a large container ship*. in *Proceedings of the 8th Asia-Pacific Workshop on Marine Hydrodynamics in Naval Architecture, Ocean Technology and Constructions, Hanoi, Vietnam*. 2016.
20. Nguyen, T., et al. *Numerical studies on air resistace reduction methods for a large container ship with fully loaded deck-containers in oblique winds*. in *MARINE VII: proceedings of the VII International Conference on Computational Methods in Marine Engineering*. 2017. CIMNE.

 doi:10.20944/preprints202509.0592.v1

21. Sugata, K., et al. *Reduction of wind force acting on Non Ballast Ship*. in *Proceedings of the 5th Asia Pacific Workshop on Marine Hydrodynamics-APHydro2010, Osaka, Japan*. 2010.